

Machine Learning Confirms GW231123 is a “Lite”-Intermediate Mass Black Hole Merger

CHAYAN CHATTERJEE ^{1,2} KAYLAH MCGOWAN ¹ SUYASH DESHMUKH ¹ AND KARAN JANI ¹

¹*Department of Physics and Astronomy, Vanderbilt University
2201 West End Avenue, Nashville, Tennessee - 37235,*

²*Data Science Institute, Vanderbilt University
1400 18th Avenue South Building, Suite 2000, Nashville, Tennessee - 37212,*

ABSTRACT

The LIGO–Virgo–KAGRA Collaboration recently reported GW231123, a black hole merger with total mass of around $190 - 265 M_{\odot}$. This event adds to the growing evidence of ‘lite’-intermediate mass black hole (IMBH) discoveries of post-merger black holes $\gtrsim 100 M_{\odot}$. GW231123 posed several data analysis challenges owing to waveform-model systematics and presence of noise artifacts called glitches. We present the first comprehensive machine learning analysis to further validate this event, strengthen its astrophysical inference, and characterize instrumental noise in its vicinity. Our approach uses a combination of tools tailored for specific analyses: GW-WHISPER, an adaptation of OpenAI’s audio transformer; ARCHGEM, a Gaussian mixture model-based soft clustering and density approximation software; and AWARE, a convolutional autoencoder. We identify the data segment containing the merger with $> 70\%$ confidence in both detectors and verify its astrophysical origin. We then characterize the scattered light glitch around the event, providing the first physically interpretable parameters for the glitch. We also reconstruct the real waveforms from the data with slightly better agreement to model-agnostic reconstructions than to quasi-circular models, hinting at possible astrophysics beyond current waveform families (such as non-circular orbits or environmental imprints). Finally, by demonstrating high-fidelity waveform reconstructions for simulated mergers with total masses between $100 - 1000 M_{\odot}$, we show that our method can confidently probe the IMBH regime. Our integrated framework offers a powerful complementary tool to traditional pipelines for rapid, robust analysis of massive, glitch-contaminated events.

1. INTRODUCTION

The gravitational wave (GW) event GW231123 (T. L. S. Collaboration et al. 2025) stands out as the most massive binary black hole (BBH) merger observed to date, with total mass in the range $190 - 265 M_{\odot}$ and unusually high spins (~ 0.9 and ~ 0.8). The event represents the latest addition to the growing catalog of low-mass or “lite” IMBH discoveries using GWs (K. Ruiz-Rocha et al. 2025; R. Udall et al. 2020; R. Abbott et al. 2020). The inferred masses of this event straddle the theorized $60 - 130 M_{\odot}$ pair instability mass gap, implying either a non-standard stellar origin or hierarchical mergers in dense environments, marking GW231123 as a critical probe of BH formation channels (I. Mandel & F. S. Broekgaarden 2022).

Accurate characterization of GW231123 has been challenging, mainly because significant waveform-model systematics have been observed between state-of-the-art inspiral–merger–ringdown (IMR) templates (V. Varma et al. 2019; G. Pratten et al. 2021; H. Estellés et al. 2022; J. E. Thompson et al. 2024; A. Ramos-Buades et al. 2023), showing divergence in the high mass, high spin regime. In addition to that, the data around the merger was contaminated by non-Gaussian transient noise artifacts (“glitches”) in both detectors. In LIGO Hanford (J. Aasi et al. 2015), a glitch related to the differential arm control loop, in a frequency range between 15 - 30 Hz had appeared at 1.1-1.7 s before the merger. This glitch was removed by using a phenomenological, wavelet-based model using the BayesWave algorithm (N. J. Cornish & T. B. Littenberg 2015; N. J. Cornish et al. 2021; M. Millhouse et al. 2018). In LIGO Livingston (J. Aasi et al. 2015), a possible scattered light glitch (B. P. Abbott et al. 2016; S. Soni et al. 2024; D. Davis

et al. 2021) was identified 2.0 - 3.0 s before the event in a frequency range between 10 - 20 Hz. Since it was determined that this glitch would have no effect on parameter inference, no subtraction was applied.

Recent studies have shown that broadband glitches that overlap with GW signals can induce significant biases in parameter estimation if coincident with the merger (J. Powell 2018; J. Y. L. Kwok et al. 2022; S. Mozzon et al. 2022; R. Macas et al. 2022; S. Hourihane et al. 2022; S. Ghonge et al. 2024). Ensuring reliable data quality is paramount for an event of such astrophysical significance, particularly because certain glitches – like Blips, Tomte, and Koi fish (B. P. Abbott et al. 2016; S. Soni et al. 2024; D. Davis et al. 2021) – can closely mimic the morphology of high-mass BBH signals. Traditional mitigation methods, relying on manual inspection and heuristic vetoes, are both labor-intensive and insufficiently scalable as detector data rates continue to climb. At the same time, the continual emergence of new glitch classes underscores the need for model-agnostic removal strategies (E. Capote et al. 2025). In this context, machine learning (ML) techniques – especially deep neural networks – offer a compelling alternative, providing automated, scalable, and broadly applicable frameworks for both noise suppression and waveform reconstruction (T. Dooney et al. 2025; B. Sánchez et al. 2019; D. George et al. 2018; S. Bahaadini et al. 2017; J. Powell et al. 2017; M. Llorens-Monteagudo et al. 2019; M. Razzano & E. Cuoco 2018; C. Chatterjee et al. 2021; P. Bacon et al. 2022).

In this work, we introduce a fully integrated ML framework tailored to high-mass, glitch-contaminated events like GW231123. Our pipeline is built around three complementary tools: GW-WHISPER (C. Chatterjee et al. 2024), an adaptation of OpenAI’s Whisper audio transformer (A. Radford et al. 2022), that processes whitened strain and performs low-latency, segment-level classification, simultaneously flagging GW signals and vetoing common glitch morphologies without human intervention. Second, we apply AWARE - Attention-boosted Waveform Reconstruction network (C. Chatterjee & K. Jani 2024a,b, 2025), a probabilistic convolutional autoencoder that generates uncertainty-aware waveform reconstructions of GW signals in the time-domain. We assess its robustness through extensive Monte-Carlo injections that embed GW231123-like signals in a range of glitch environments and extend to binary mergers with total masses from 100 to 1000 M_{\odot} . Finally, ARCHGEM (K. B. McGowan et al. 2025) employs Gaussian-mixture clustering on Q-transform spectrograms to isolate scattered-light arches and derive physically meaningful parameters – such as recurrence frequency, displacement, and velocity – providing actionable feedback for detector commissioning. Together, these components form a rapid and scalable pipeline that complements traditional matched filter (L. S. Finn 2001) and Bayesian analyses, enabling more reliable signal validation and noise characterization for current and future observations of IMBH mergers.

This paper is organized as follows: Section 2 describes results obtained using GW-WHISPER on 8 seconds of whitened data around the event. Section 3 explores scattered light glitch characterization around GW231123 using ARCHGEM with comparisons against trends observed across the O4 observation run. Section 4 presents analyses performed using AWARE on GW231123 data and simulated injection sets that span a wide range of IMBH masses. We present our conclusions in Section 5.

2. SIGNAL CLASSIFICATION

We use GW-WHISPER (C. Chatterjee et al. 2024) to classify and tag glitches and GW events present in 8 s of data around the merger time of GW231123. GW-WHISPER builds on OpenAI’s Whisper audio transformer architecture (A. Radford et al. 2022), originally trained on 680,000 hours of audio data. Chatterjee et al. (C. Chatterjee et al. 2024) showed that it is possible to adapt Whisper for GW data analysis by fine-tuning only $\sim 0.5\%$ of the parameters of the pre-trained Whisper encoder on GW injections and glitch data. This was achieved using a parameter-efficient finetuning (L. Xu et al. 2023) technique called DoRA (Weight-decomposed Low Rank Adaptation) (S.-Y. Liu et al. 2024), which has gained popularity in large language model (LLM) applications. In order to perform GW and glitch classification, GW-WHISPER was trained on a curated set of glitches from the GravitySpy catalog (M. Zevin et al. 2017) with similar morphology to high-mass GW events: Blip, Low-Frequency Blip, Koi Fish, and Tomte, and a simulated set of BBH mergers with total mass $> 50M_{\odot}$ injected into background O3 data. An additional “No Glitch” class was included to represent background segments without prominent glitches or GW signals (see Fig. 4(c) in C. Chatterjee et al. (2024) for reference).

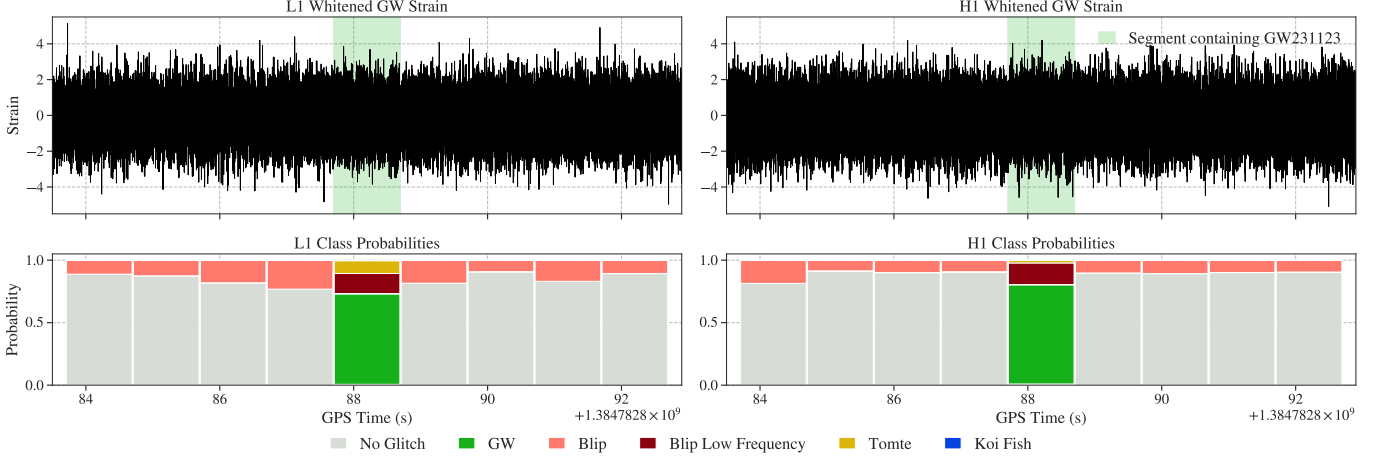


Figure 1. Predicted class label probabilities from 8 seconds around GW231123 using GW-WHISPER in Livingston (left) and Hanford (right). The top row shows the whitened strains from the respective detectors with the segment containing the event highlighted green. The bottom row contains the probabilities for each label in each segment. The model predicts “No Glitch” for all segments around the event and “GW” in the segment that contains the event.

We employ this trained model to identify GW231123 and surrounding glitches. The model takes as input log-mel spectrogram representations of single-detector, whitened, 1 s strain segments and outputs a probability distribution over the aforementioned set of GW+glitch classes for each segment. Fig. 1 shows the model outputs for 8 s data surrounding GW231123. In Hanford and Livingston data, GW-WHISPER identifies the segment containing the signal with a confidence of 79.32% and 72.33% respectively. All other segments are consistently classified as “No Glitch” with high confidence (there is a small residual probability in these segments and we find that they are predominantly assigned to the “Blip” class). Although both detectors contained low-frequency glitches near the time of the event, these transients were removed by the 20 Hz high-pass filter applied in the data preprocessing step. This filtering step matches the processing used for generating the training dataset, and is intended to remove the low-frequency noise component in the data, enabling the model to better focus on GW events.

3. SCATTERED LIGHT GLITCH CHARACTERIZATION

To investigate low-frequency scattering noise in aLIGO preceding the GW23123 event, we applied the ARCHGEM software to strain data from the Livingston interferometer, using the calibrated channel `L1:GDS-CALIB-STRAIN.CLEAN.AR`. Our analysis focused on a 18 second window centered on GPS time 1384782888. The upper panel of Fig. 2 presents the resulting Q-transform spectrogram, which displays a series of arch-like features below 40 Hz, typical of scattered light artifacts caused by moving surfaces coupling into the main interferometric beam path. We used a two-pronged analysis to isolate and characterize these arches. First, we employed a peak-finding algorithm to extract the local maxima in frequency over time for high-energy pixels. Second, we applied Gaussian Mixture Modeling (GMM) with 9 components to cluster time-frequency-energy points and identify statistically distinct groupings of noise activity. Both methods included a post-processing filter to retain only the most temporally distinct peaks. The lower panel of Fig. 2 overlays the retained peaks from both methods. The “Find Peaks” method identified several high-confidence features, yielding an average maximum arch frequency of $f_{\text{max,avg}} = 14.36$ Hz. The GMM method identified centroids clustered around lower frequencies, with a corresponding average of $f_{\text{max,avg}} = 11.13$ Hz.

From the distribution of the retained peak times, we can infer a scattering recurrence frequency of $f_{\text{scat}} = 0.19$ Hz, indicating a periodic process consistent with a surface oscillating at low frequency. Using the measured f_{scat} , we calculated a scattering surface displacement of $x_{\text{surf}} = 0.11 \mu\text{m}$ and an average surface velocity of $v_{\text{surf,avg}} = 0.41 \mu\text{m/s}$. We also report a standard deviation in peak frequency of $\sigma_f = 1.55$ Hz, while the inter-peak time intervals were temporally coherent with $\sigma_{\Delta t} = 0.00$ s, suggesting highly periodic motion. Notably the $f_{\text{max,avg}}$ for this scattering event is lower than the average distribution seen in ArchGEM’s O4 scattered light study (K. B. McGowan et al. 2025). Though we can only infer that the glitch classification is scattering, due to there only being 2 cycles, these

results validate ARCHGEM’s ability to extract physically meaningful scattering parameters from non-linear noise features in GW strain data. The combination of clustering and peak-tracking approaches enhances robustness and interpretability, particularly for characterizing complex noise morphologies near GW event times.

4. WAVEFORM RECONSTRUCTION

In previous studies, the feasibility of AWARE was demonstrated for waveform reconstructions of real GW events (C. Chatterjee & K. Jani 2024a). To obtain the results in this study, we trained a new version of AWARE on simulated BBHs with total masses between 100 and 1000 M_\odot in the detector frame. These signals were injected into random segments of background data around GW231123, excluding the event time. In our new model architecture, we replace the simple convolutional encoder and Long Short Term Memory (LSTM) (S. Hochreiter & J. Schmidhuber 1997) decoder in the original model architecture with purely convolutional U-Net (O. Ronneberger et al. 2015) encoder and decoder. The encoder U-Net consists of three levels of 1D convolutional blocks (Y. Lecun et al. 1998; A. Krizhevsky et al. 2012), with a multi-head self-attention module (A. Vaswani et al. 2017) at the narrowest “bottleneck” layer, that produces a low-dimensional representation of the input. The signal is then rebuilt to its original length (with noise subtracted) using learned up-scaling convolutional layers in the decoder U-Net. Instead of outputting a single waveform, the network predicts, for each time sample, the mean and spread of a Gaussian. The final reconstruction is thus a sum of independent Gaussian random variables, providing a best-estimate waveform with its associated reconstruction uncertainty.

The red dashed curves in Fig. 3 (a) and (b) show the mean AWARE reconstructions, and the variances of the Gaussians are used to obtain the reconstruction uncertainty (red bands). For comparisons, we plot the waveform-model agnostic cWB reconstructions (green) (S. Klimenko et al. 2016), reconstructions from NRSur7dq4 waveform-model parameter estimation results using the software package, Bilby (G. Ashton et al. 2019) (blue) and wavelet-based reconstruction algorithm BayesWave (N. J. Cornish & T. B. Littenberg 2015; N. J. Cornish et al. 2021; M. Millhouse et al. 2018) (purple). We observe excellent amplitude and phase consistency between AWARE reconstructions and the other approaches. For the Hanford (Livingston) signal, the mean AWARE reconstruction shows overlaps of 92% (97%),

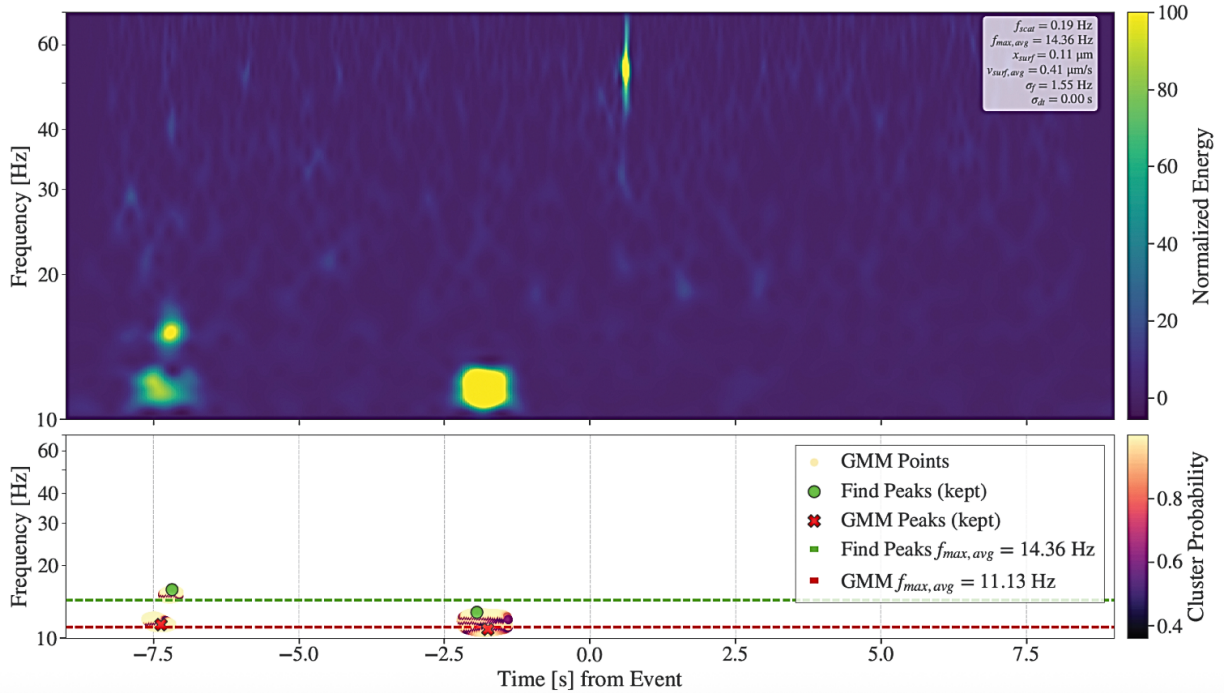


Figure 2. The top panel displays the Q-transform visualization of the GW231123 event and scattered light glitches observed at the Livingston Observatory. The bottom panel is the ARCHGEM output highlighting the software’s capability to recognize scattered light morphology and extract them for further analysis using a dual methodology ML approach.

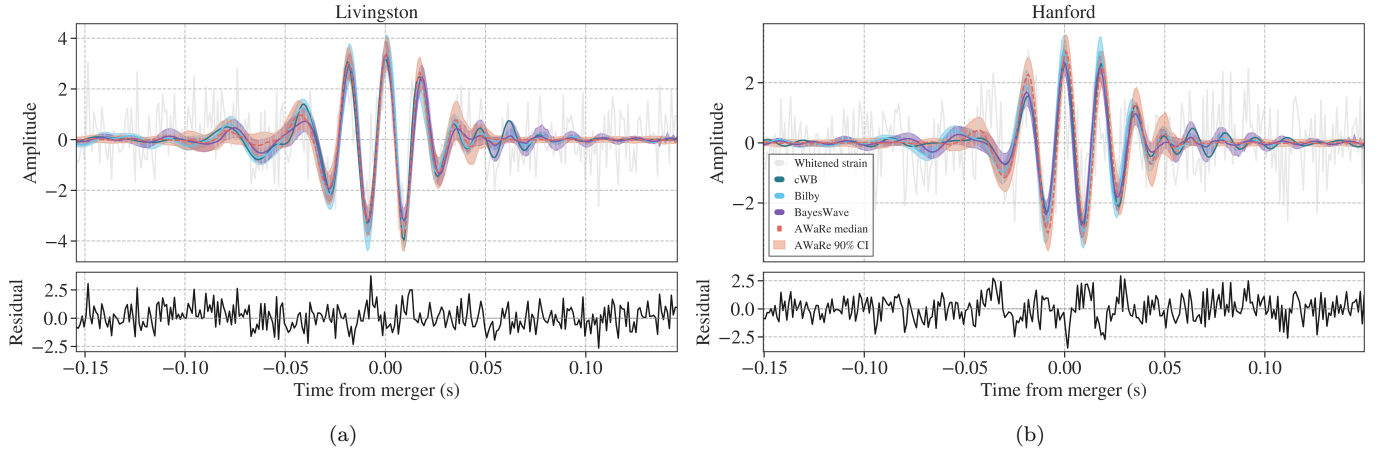


Figure 3. Top: Reconstructions of (a) Livingston and (b) Hanford data of GW231123 using AWaRe. The red dashed curves shows the AWaRe mean reconstructions. The red bands show the associated reconstruction uncertainties. Reconstructions from cWB, Bilby and BayesWave are shown in green, blue and purple respectively. The whitened noisy strains are shown in grey. Bottom: Residuals obtained by subtracting the AWaRe mean reconstructions from the whitened strains.

91% (97%) and 96% (98%) with cWB (S. Klimenko et al. 2016), Bilby (G. Ashton et al. 2019) and BayesWave (N. J. Cornish & T. B. Littenberg 2015; N. J. Cornish et al. 2021; M. Millhouse et al. 2018) reconstructions respectively, indicating high accuracy. The slightly stronger agreement with the template-free cWB and BayesWave methods – compared with the template-based Bilby result – suggests that AWaRe captures intrinsic signal morphology that is robust to waveform-model systematics.

In the bottom panel of Fig. 3, we plot the residuals obtained by subtracting the AWaRe mean reconstructions from the noisy strain data. For perfect reconstruction, the residuals would be normally distributed. After obtaining the residuals, we inspect their normality by performing the Shapiro-Wilk test (S. S. Shapiro & M. B. Wilk 1965) on the residuals of Hanford and Livingston data and computing its p-value. Lower p-values indicate a lower probability that the coherent power in the residuals is due to instrumental noise alone. We obtain p-values of 0.671 for Hanford and 0.454 for Livingston residuals. Since both values are > 0.05 , the test indicates strong evidence that the residuals follow the expected normal distribution. The optimal SNRs of the residuals in Hanford and Livingston were found to be 0.82 and 0.55, further supporting our findings that subtracting the reconstruction from the original strain leaves negligible residual power.

Next, we performed tests on simulated GW231123-like waveforms injected in noise background around the event. These waveforms were generated using Bilby posterior samples obtained using the following waveform approximants: NRSur7dq4 (V. Varma et al. 2019), IMRPhenomXPHM (G. Pratten et al. 2021), IMRPhenomTPHM (H. Estellés et al. 2022), IMRPhenomXO4a (J. E. Thompson et al. 2024), SEOBNRv5PHM (A. Ramos-Buades et al. 2023). The network SNR of these injections were fixed at the reported value, i.e., 22.6. In Fig. 4 (a), we plot the overlap distributions between 500 simulated GW231123-like waveforms and their AWaRe reconstructions in Hanford and Livingston data. For all the models, the distributions peak at overlap values > 0.90 , indicating high reconstruction consistency between injected and recovered waveforms.

We also tested the performance for signals randomly injected in 1 s O3 data segments containing glitches. The motivation of this study was to test the robustness of AWaRe reconstructions in the presence of morphologically-similar glitches. We injected synthetic GW231123 signals from the NRSur7dq4 model into O3 strain segments containing seven common glitch morphologies (Blip, Koi-fish, Tomte, Low-frequency burst, Repeating blips, Whistle, and Scattered light). Since AWaRe is trained to isolate and reconstruct only the astrophysical waveform, the model yields overlap distributions sharply peaked near 1.0 for all glitch types, demonstrating its capacity to remove diverse non-Gaussian artifacts and recover the true signal with high fidelity (Fig. 4 (b)). Small broadening of the peaks for Tomte and Koi-fish glitches reflects slightly greater reconstruction uncertainty when these morphologies overlap the

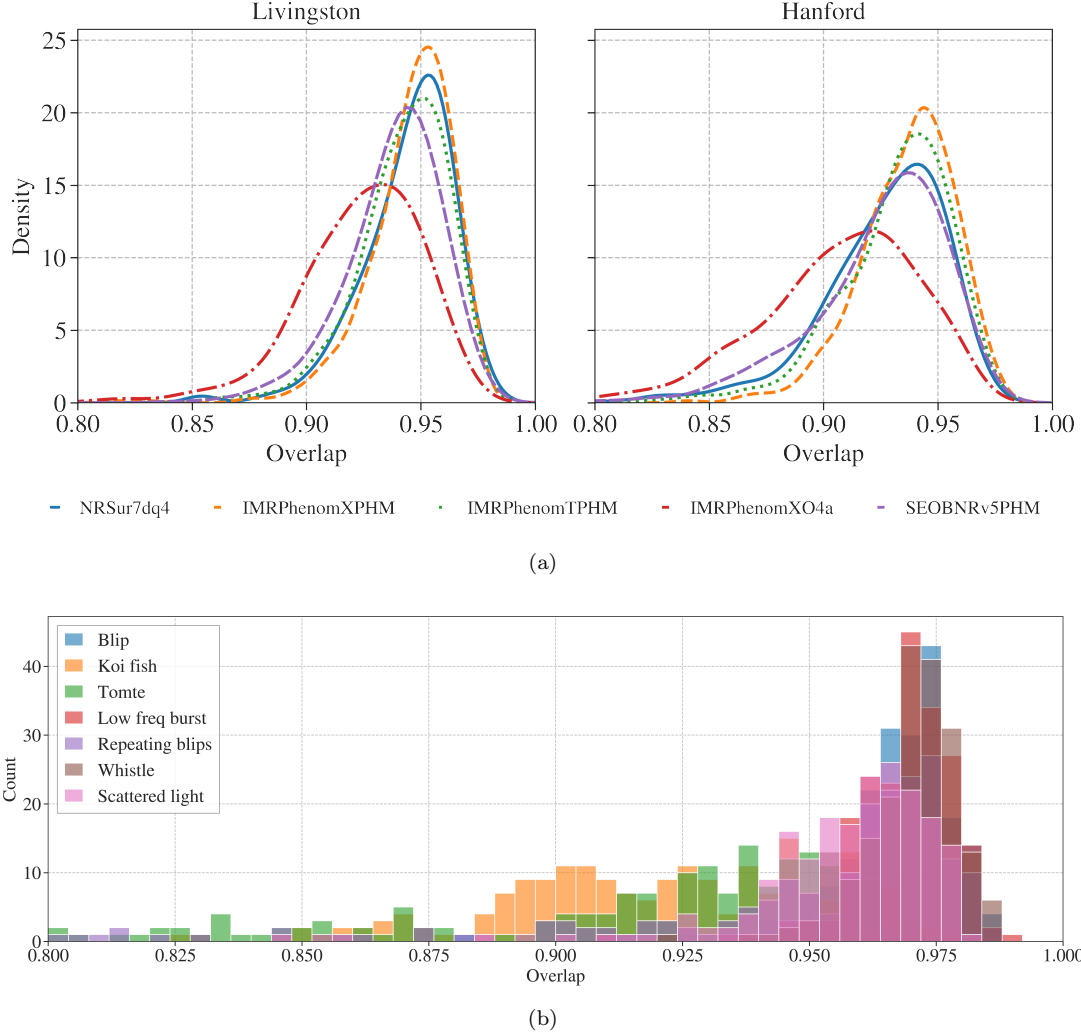


Figure 4. (a) Overlap distributions between GW231123-like waveforms in Hanford and Livingston generated from posterior samples of various approximants and their AWARE reconstructions. (b) Overlap distributions between AWARE reconstructions and GW231123-like injections in O3 noise contaminated by different glitches.

signal’s time–frequency support. These results further demonstrate how AWARE is complementary to GW-Whisper and ArchGEM: while GW-Whisper excels at identifying the presence of a signal and classifying common glitch types, and ArchGEM specializes in characterizing scattered-light artifacts, AWARE is trained to isolate and reconstruct only the astrophysical waveform, allowing it to recover true GW signals even in the presence of any glitch morphology.

To test whether the AWARE reconstruction pipeline generalizes beyond a single extreme event, we generated an injection set of BBH signals with total masses $100 - 1000M_{\odot}$ and $\text{SNR}=15$, and obtained their reconstructions using AWARE. The chosen mass range spans the crucial pair-instability gap and the lower IMBH population, where signals are short, templates disagree, and glitches can masquerade as mergers. Fig. 5 shows box plots of overlap between reconstructions and true waveforms in $100M_{\odot}$ bins. We find that the medians remain high (> 0.9) up to $500M_{\odot}$, then gradually fall toward ~ 0.85 with broader interquartile ranges at higher masses, reflecting the increasing difficulty of recovering merger–ringdown–dominated signals in noisy data. Even in the $900 - 1000M_{\odot}$ bin, most overlaps exceed 0.8, indicating substantial fidelity. These results demonstrate that AWARE can rapidly and reliably vet candidate IMBH mergers and quantifies where waveform systematics and non-Gaussian noise begin to erode accuracy.

5. CONCLUSIONS

We have presented the first ML follow-up of the BBH merger GW231123. Our integrated pipeline, comprising GW-WHISPER for low-latency segment classification, ARCHGEM for scattered-light glitch diagnostics, and AWARE for probabilistic waveform reconstruction addresses simultaneously the dual challenges that defined this event: strong waveform-model systematics and nearby non-Gaussian noise transients. GW-WHISPER autonomously flags the merger without human vetting. ARCHGEM extracts physically interpretable parameters of the Livingston scattered-light arches, providing actionable feedback for detector commissioning. AWARE produces reconstructions that agree more closely with template-free cWB and BayesWave results than with template-based Bilby posteriors. Injection studies covering seven common glitch morphologies and an extended mass range of $100\text{--}1000 M_\odot$ show that AWARE retains high fidelity across the lower-mass IMBH regime, and quantifies the onset of accuracy loss for the heaviest systems. We show that if an even higher mass merger is detected, our pipelines are capable of identifying and characterize its signal and noise properties. AWARE reconstructions, in particular, could allow us to probe the astrophysics of such systems upto $1000 M_\odot$. Complementing the signal analyses, as detector sensitivity improves and glitch diversity grows, such ML-driven frameworks will be essential for maximising the astrophysical return from the most challenging GW sources.

ACKNOWLEDGMENTS

The authors would like to thank Tabata Ferreira for helpful comments and suggestions. This research was undertaken with the support of compute grant and resources, particularly the DGX A100 AI Computing Server, offered by the Vanderbilt Data Science Institute (DSI) located at Vanderbilt University, USA. This research used data obtained from the Gravitational Wave Open Science Center (<https://www.gw-openscience.org>), a service of LIGO Laboratory, the LIGO Scientific Collaboration and the Virgo Collaboration. LIGO is funded by the U.S. National Science Foundation. Virgo is funded by the French Centre National de Recherche Scientifique (CNRS), the Italian Istituto Nazionale della Fisica Nucleare (INFN) and the Dutch Nikhef, with contributions by Polish and Hungarian institutes. This material is based upon work supported by NSF’s LIGO Laboratory which is a major facility fully funded by the National Science Foundation.

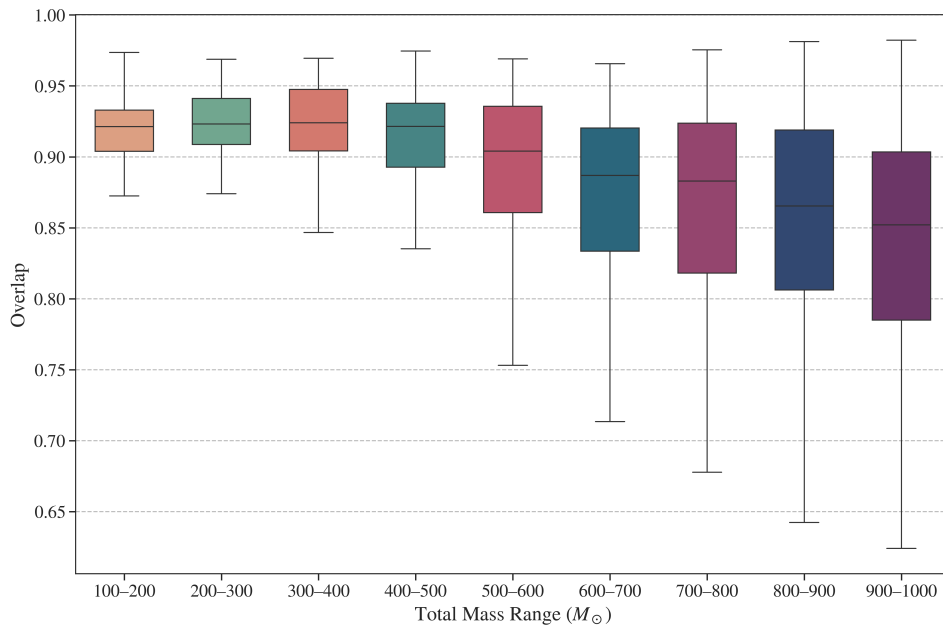


Figure 5. Box plots showing the median and interquartile ranges of the overlap distributions between AWARE reconstructions and original waveforms for simulated BBH events with total masses between $100 - 1000 M_\odot$.

REFERENCES

- Aasi, J., Abbott, B. P., Abbott, R., et al. 2015, *Classical and Quantum Gravity*, 32, 074001, doi: [10.1088/0264-9381/32/7/074001](https://doi.org/10.1088/0264-9381/32/7/074001)
- Abbott, B. P., Abbott, R., Abbott, T. D., et al. 2016, *Classical and Quantum Gravity*, 33, 134001, doi: [10.1088/0264-9381/33/13/134001](https://doi.org/10.1088/0264-9381/33/13/134001)
- Abbott, R., Abbott, T. D., Abraham, S., et al. 2020, *Phys. Rev. Lett.*, 125, 101102, doi: [10.1103/PhysRevLett.125.101102](https://doi.org/10.1103/PhysRevLett.125.101102)
- Ashton, G., Hübner, M., Lasky, P. D., et al. 2019, *The Astrophysical Journal Supplement Series*, 241, 27, doi: [10.3847/1538-4365/ab06fc](https://doi.org/10.3847/1538-4365/ab06fc)
- Bacon, P., Trovato, A., & Bejger, M. 2022, Denoising gravitational-wave signals from binary black holes with dilated convolutional autoencoder, <https://arxiv.org/abs/2205.13513>
- Bahaadini, S., Rohani, N., Coughlin, S., et al. 2017, *Deep Multi-view Models for Glitch Classification*, <https://arxiv.org/abs/1705.00034>
- Capote, E., Jia, W., Aritomi, N., et al. 2025, *Phys. Rev. D*, 111, 062002, doi: [10.1103/PhysRevD.111.062002](https://doi.org/10.1103/PhysRevD.111.062002)
- Chatterjee, C., & Jani, K. 2024a, *The Astrophysical Journal*, 969, 25, doi: [10.3847/1538-4357/ad4602](https://doi.org/10.3847/1538-4357/ad4602)
- Chatterjee, C., & Jani, K. 2024b, *The Astrophysical Journal*, 973, 112, doi: [10.3847/1538-4357/ad6984](https://doi.org/10.3847/1538-4357/ad6984)
- Chatterjee, C., & Jani, K. 2025, *Astrophys. J.*, 982, 102, doi: [10.3847/1538-4357/adbb66](https://doi.org/10.3847/1538-4357/adbb66)
- Chatterjee, C., Wen, L., Diakogiannis, F., & Vinsen, K. 2021, *Phys. Rev. D*, 104, 064046, doi: [10.1103/PhysRevD.104.064046](https://doi.org/10.1103/PhysRevD.104.064046)
- Chatterjee, C., Petulante, A., Jani, K., et al. 2024, Pre-trained Audio Transformer as a Foundational AI Tool for Gravitational Waves, *arXiv*, doi: [10.48550/arXiv.2412.20789](https://doi.org/10.48550/arXiv.2412.20789)
- Collaboration, T. L. S., the Virgo Collaboration, & the KAGRA Collaboration. 2025, GW231123: a Binary Black Hole Merger with Total Mass 190-265 M_{\odot} , <https://arxiv.org/abs/2507.08219>
- Cornish, N. J., & Littenberg, T. B. 2015, *Classical and Quantum Gravity*, 32, 135012, doi: [10.1088/0264-9381/32/13/135012](https://doi.org/10.1088/0264-9381/32/13/135012)
- Cornish, N. J., Littenberg, T. B., Bécsy, B., et al. 2021, *Phys. Rev. D*, 103, 044006, doi: [10.1103/PhysRevD.103.044006](https://doi.org/10.1103/PhysRevD.103.044006)
- Davis, D., Areeda, J. S., Berger, B. K., et al. 2021, *Classical and Quantum Gravity*, 38, 135014, doi: [10.1088/1361-6382/abfd85](https://doi.org/10.1088/1361-6382/abfd85)
- Dooney, T., Narola, H., Bromuri, S., et al. 2025, *Phys. Rev. D*, 112, 044022, doi: [10.1103/s91m-c2jw](https://doi.org/10.1103/s91m-c2jw)
- Estellés, H., Colleoni, M., García-Quirós, C., et al. 2022, *Phys. Rev. D*, 105, 084040, doi: [10.1103/PhysRevD.105.084040](https://doi.org/10.1103/PhysRevD.105.084040)
- Finn, L. S. 2001, *Phys. Rev. D*, 63, 102001, doi: [10.1103/PhysRevD.63.102001](https://doi.org/10.1103/PhysRevD.63.102001)
- George, D., Shen, H., & Huerta, E. A. 2018, *Phys. Rev. D*, 97, 101501, doi: [10.1103/PhysRevD.97.101501](https://doi.org/10.1103/PhysRevD.97.101501)
- Ghonge, S., Brandt, J., Sullivan, J. M., et al. 2024, Assessing and Mitigating the Impact of Glitches on Gravitational-Wave Parameter Estimation: a Model Agnostic Approach, <https://arxiv.org/abs/2311.09159>
- Hochreiter, S., & Schmidhuber, J. 1997, *Neural Computation*, 9, 1735
- Hourihane, S., Chatziioannou, K., Wijngaarden, M., et al. 2022, *Phys. Rev. D*, 106, 042006, doi: [10.1103/PhysRevD.106.042006](https://doi.org/10.1103/PhysRevD.106.042006)
- Klimenko, S., Vedovato, G., Drago, M., et al. 2016, *Phys. Rev. D*, 93, 042004, doi: [10.1103/PhysRevD.93.042004](https://doi.org/10.1103/PhysRevD.93.042004)
- Krizhevsky, A., Sutskever, I., & Hinton, G. E. 2012, in *Advances in Neural Information Processing Systems*, ed. F. Pereira, C. Burges, L. Bottou, & K. Weinberger, Vol. 25 (Curran Associates, Inc.)
- Kwok, J. Y. L., Lo, R. K. L., Weinstein, A. J., & Li, T. G. F. 2022, *Phys. Rev. D*, 105, 024066, doi: [10.1103/PhysRevD.105.024066](https://doi.org/10.1103/PhysRevD.105.024066)
- Lecun, Y., Bottou, L., Bengio, Y., & Haffner, P. 1998, *Proceedings of the IEEE*, 86, 2278, doi: [10.1109/5.726791](https://doi.org/10.1109/5.726791)
- Liu, S.-Y., Wang, C.-Y., Yin, H., et al. 2024, DoRA: Weight-Decomposed Low-Rank Adaptation, <https://arxiv.org/abs/2402.09353>
- Llorens-Monteagudo, M., Torres-Forné, A., Font, J. A., & Marquina, A. 2019, *Classical and Quantum Gravity*, 36, 075005, doi: [10.1088/1361-6382/ab0657](https://doi.org/10.1088/1361-6382/ab0657)
- Macas, R., Pooley, J., Nuttall, L. K., et al. 2022, *Phys. Rev. D*, 105, 103021, doi: [10.1103/PhysRevD.105.103021](https://doi.org/10.1103/PhysRevD.105.103021)
- Mandel, I., & Broekgaarden, F. S. 2022, *Living Rev. Rel.*, 25, 1, doi: [10.1007/s41114-021-00034-3](https://doi.org/10.1007/s41114-021-00034-3)
- McGowan, K. B., et al. 2025, in prep for arXiv e-prints
- Millhouse, M., Cornish, N. J., & Littenberg, T. 2018, *Phys. Rev. D*, 97, 104057, doi: [10.1103/PhysRevD.97.104057](https://doi.org/10.1103/PhysRevD.97.104057)
- Mozzon, S., Ashton, G., Nuttall, L. K., & Williamson, A. R. 2022, *Physical Review D*, 106, doi: [10.1103/physrevd.106.043504](https://doi.org/10.1103/physrevd.106.043504)
- Powell, J. 2018, *Classical and Quantum Gravity*, 35, 155017, doi: [10.1088/1361-6382/aacf18](https://doi.org/10.1088/1361-6382/aacf18)
- Powell, J., Torres-Forné, A., Lynch, R., et al. 2017, *Classical and Quantum Gravity*, 34, 034002, doi: [10.1088/1361-6382/34/3/034002](https://doi.org/10.1088/1361-6382/34/3/034002)

- Pratten, G., García-Quirós, C., Colleoni, M., et al. 2021, Phys. Rev. D, 103, 104056, doi: [10.1103/PhysRevD.103.104056](https://doi.org/10.1103/PhysRevD.103.104056)
- Radford, A., Kim, J. W., Xu, T., et al. 2022, Robust Speech Recognition via Large-Scale Weak Supervision, <https://arxiv.org/abs/2212.04356>
- Ramos-Buades, A., Buonanno, A., Estellés, H., et al. 2023, Phys. Rev. D, 108, 124037, doi: [10.1103/PhysRevD.108.124037](https://doi.org/10.1103/PhysRevD.108.124037)
- Razzano, M., & Cuoco, E. 2018, Classical and Quantum Gravity, 35, 095016, doi: [10.1088/1361-6382/aab793](https://doi.org/10.1088/1361-6382/aab793)
- Ronneberger, O., Fischer, P., & Brox, T. 2015, CoRR, abs/1505.04597
- Ruiz-Rocha, K., Yelkar, A. B., Lange, J., et al. 2025, Astrophys. J. Lett., 985, L37, doi: [10.3847/2041-8213/adc5f8](https://doi.org/10.3847/2041-8213/adc5f8)
- Shapiro, S. S., & Wilk, M. B. 1965, Biometrika, 52, 591. <http://www.jstor.org/stable/2333709>
- Soni, S., Berger, B. K., Davis, D., et al. 2024, LIGO Detector Characterization in the first half of the fourth Observing run, <https://arxiv.org/abs/2409.02831>
- Sánchez, B., Domínguez R., M., Lares, M., et al. 2019, Astronomy and Computing, 28, 100284, doi: <https://doi.org/10.1016/j.ascom.2019.05.002>
- Thompson, J. E., Hamilton, E., London, L., et al. 2024, Phys. Rev. D, 109, 063012, doi: [10.1103/PhysRevD.109.063012](https://doi.org/10.1103/PhysRevD.109.063012)
- Udall, R., Jani, K., Lange, J., et al. 2020, Astrophys. J., 900, 80, doi: [10.3847/1538-4357/abab9d](https://doi.org/10.3847/1538-4357/abab9d)
- Varma, V., Field, S. E., Scheel, M. A., et al. 2019, Phys. Rev. Res., 1, 033015, doi: [10.1103/PhysRevResearch.1.033015](https://doi.org/10.1103/PhysRevResearch.1.033015)
- Vaswani, A., Shazeer, N., Parmar, N., et al. 2017, CoRR, abs/1706.03762
- Xu, L., Xie, H., Qin, S.-Z. J., Tao, X., & Wang, F. L. 2023, Parameter-Efficient Fine-Tuning Methods for Pretrained Language Models: A Critical Review and Assessment, <https://arxiv.org/abs/2312.12148>
- Zevin, M., Coughlin, S., Bahaadini, S., et al. 2017, Classical and Quantum Gravity, 34, 064003, doi: [10.1088/1361-6382/aa5cea](https://doi.org/10.1088/1361-6382/aa5cea)